

Electronic Supplementary Information (ESI)

**Enhancing Effect of Bisulfite on Sequestration of
Selenite by Zerovalent Iron**

Jinxiang Li,^{a‡} Chao Wang,^{a‡} Junlian Qiao,^{*a} Hejie Qin^{ab} and Lina Li^b

^aState Key Laboratory of Pollution Control and Resources Reuse, College of Environmental Science and Engineering, Tongji University, Shanghai 200092, People's Republic of China

^bShanghai Synchrotron Radiation Facility, Shanghai Institute of Applied Physics, Chinese Academy of Sciences, Shanghai 201204, People's Republic of China

[‡]Authors contributed equally to this work.

E-mail addresses: ljx870616@126.com (J.X. Li), wangchao962@163.com (C. Wang), qiaoqiao@tongji.edu.cn (J.L. Qiao), chinhj@foxmail.com (H.J. Qin), lilina@sinap.ac.cn (L.N. Li)

*Author to whom correspondence should be addressed

Junlian Qiao, email: qiaoqiao@tongji.edu.cn; phone: +86-021-65489163

Number of pages (including this page): 11

Number of Figures: 7

Summary

Figure S1. SEM (a), particle size distribution (b) and Raman spectra (c) of the pristine ZVI employed in this study. (Page S4)

Figure S2. The effect of HSO_3^- on the transformation of Se(IV). Reaction conditions: $[\text{Se(IV)}]_0 = 10.0 \text{ mg L}^{-1}$, $[\text{HSO}_3^-]_0 = 2.0 \text{ mM}$, $[\text{pH}]_{\text{ini}} = 5.0$, $V_{\text{air}} = 2.0 \text{ mL}$. (Page S5)

Figure S3. Correlation of Se(IV) removal rate with the headspace (V_{air}) in the presence of SO_4^{2-} . Reaction conditions: $[\text{Fe}^0] = 2.0 \text{ mM}$, $[\text{Se(IV)}]_0 = 10.0 \text{ mg L}^{-1}$, $[\text{SO}_4^{2-}]_0 = 2.0 \text{ mM}$, $\text{pH}_{\text{ini}} = 5.0$. (Page S6)

Figure S4. Correlation of Se(IV) removal rate with the headspace (V_{air}) in the presence of HSO_3^- . Reaction conditions: $[\text{Fe}^0] = 2.0 \text{ mM}$, $[\text{Se(IV)}]_0 = 10.0 \text{ mg L}^{-1}$, $[\text{HSO}_3^-]_0 = 2.0 \text{ mM}$, $\text{pH}_{\text{ini}} = 5.0$. (Page S7)

Figure S5. SEM images of the Se(IV)-treated ZVI corrosion products with the presence of SO_4^{2-} or HSO_3^- at different reaction time. Reaction conditions: $[\text{Fe}^0] = 2.0 \text{ mM}$, $[\text{Se(IV)}]_0 = 10.0 \text{ mg L}^{-1}$, $[\text{SO}_4^{2-}/\text{HSO}_3^-]_0 = 2.0 \text{ mM}$, $\text{pH}_{\text{ini}} = 5.0$, $V_{\text{air}} = 2.0 \text{ mL}$. (Page S8)

Figure S6. Theoretical calculation of the distribution of Se(IV) at variable pH. (Page S9)

Figure S7. Variations in dissolved Fe(II) and pH during Se(IV) removal by ZVI at various pH_{ini} levels. Reaction conditions: $[\text{Fe}^0] = 2.0 \text{ mM}$, $[\text{Se(IV)}]_0 = 10.0 \text{ mg L}^{-1}$, $[\text{HSO}_3^-/\text{SO}_4^{2-}]_0 = 2.0 \text{ mM}$, $V_{\text{air}} = 2.0 \text{ mL}$. (Page S10)

Table S1. Speciation of Fe in Se(IV)-treated ZVI corrosion products based on LCF of

Fe k^3 -weighted EXAFS spectra (Data were given as % values). (Page S11)

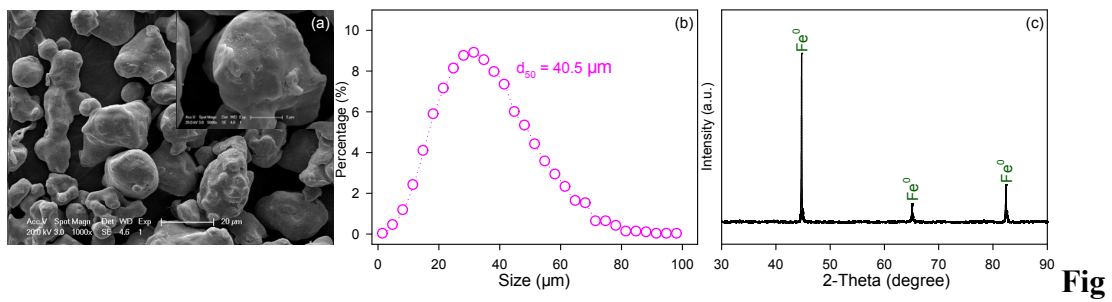


Figure S1. SEM (a), particle size distribution (b) and XRD (c) of the pristine ZVI employed in this study.

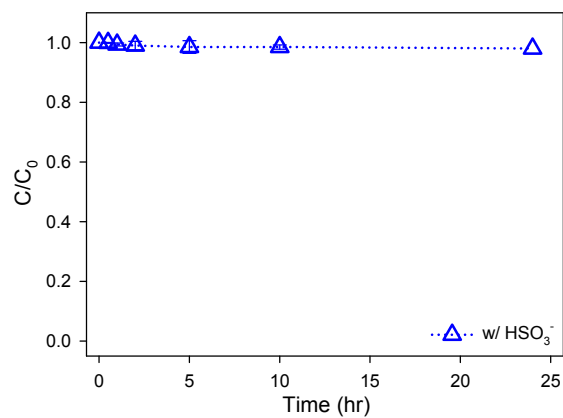


Figure S2. The effect of HSO_3^- on the transformation of Se(IV). Reaction conditions:

$[\text{Se(IV)}]_0 = 10.0 \text{ mg L}^{-1}$, $[\text{HSO}_3^-]_0 = 2.0 \text{ mM}$, $[\text{pH}]_{\text{ini}} = 5.0$, $V_{\text{air}} = 2.0 \text{ mL}$.

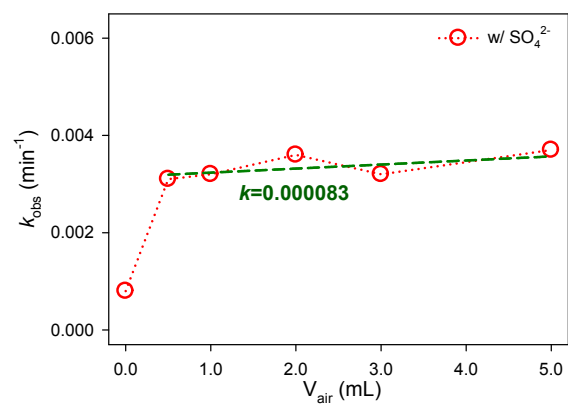


Figure S3. Correlation of Se(IV) removal rate with the headspace (V_{air}) in the presence of SO_4^{2-} . Reaction conditions: $[\text{Fe}^0] = 2.0 \text{ mM}$, $[\text{Se(IV)}]_0 = 10.0 \text{ mg L}^{-1}$, $[\text{SO}_4^{2-}]_0 = 2.0 \text{ mM}$, $\text{pH}_{\text{ini}} = 5.0$.

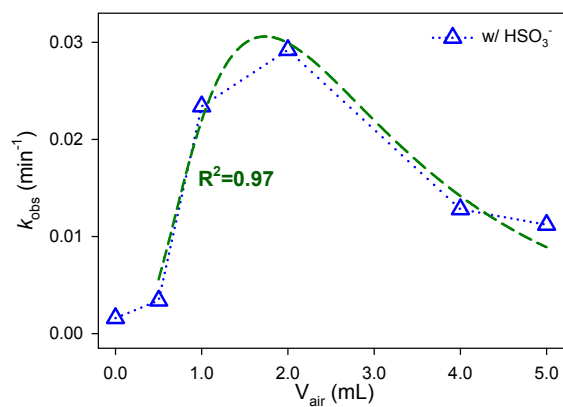


Figure S4. Correlation of Se(IV) removal rate with the headspace (V_{air}) in the presence of HSO_3^- . Reaction conditions: $[\text{Fe}^0] = 2.0 \text{ mM}$, $[\text{Se(IV)}]_0 = 10.0 \text{ mg L}^{-1}$, $[\text{HSO}_3^-]_0 = 2.0 \text{ mM}$, $\text{pH}_{\text{ini}} = 5.0$.

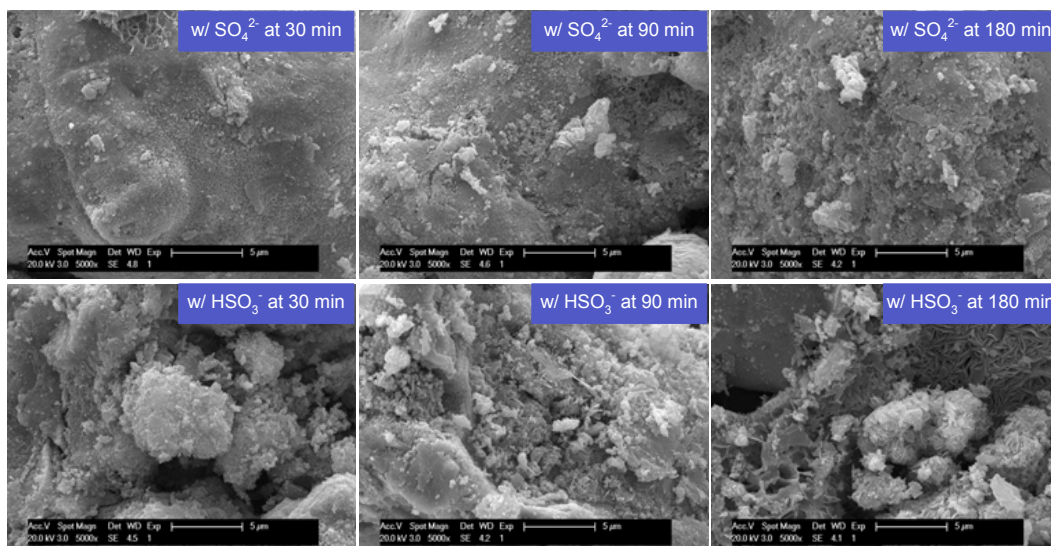


Figure S5. SEM images of the Se(IV)-treated ZVI corrosion products with the presence of SO_4^{2-} or HSO_3^- at different reaction time. Reaction conditions: $[\text{Fe}^0] = 2.0$ mM, $[\text{Se(IV)}]_0 = 10.0$ mg L^{-1} , $[\text{SO}_4^{2-}/\text{HSO}_3^-]_0 = 2.0$ mM, $\text{pH}_{\text{ini}} = 5.0$, $V_{\text{air}} = 2.0$ mL.

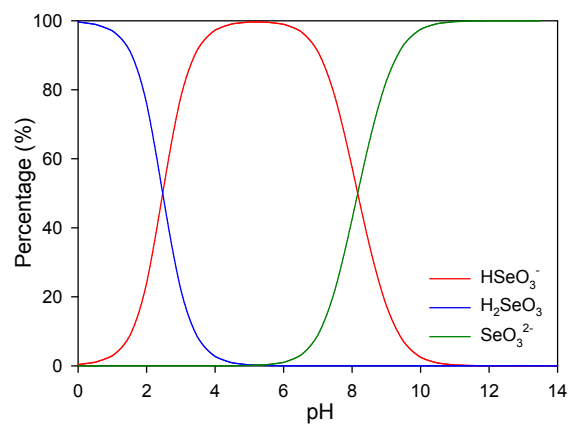


Figure S6. Theoretical calculation of the distribution of Se(IV) at variable pH.

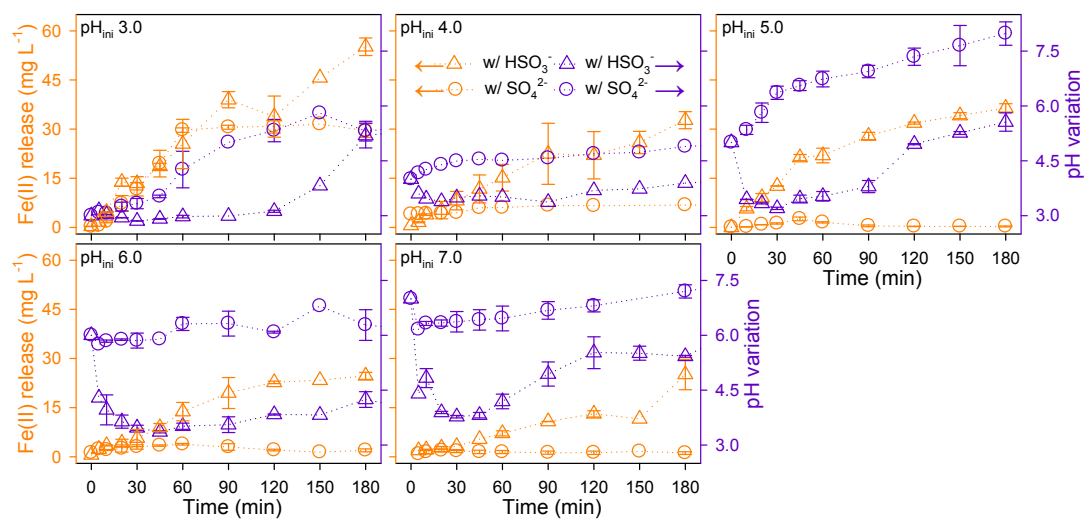


Figure S7. Variations in dissolved Fe(II) and pH during Se(IV) removal by ZVI at various pH_{ini} levels. Reaction conditions: $[\text{Fe}^0] = 2.0 \text{ mM}$, $[\text{Se(IV)}]_0 = 10.0 \text{ mg L}^{-1}$, $[\text{HSO}_3^-/\text{SO}_4^{2-}]_0 = 2.0 \text{ mM}$, $V_{\text{air}} = 2.0 \text{ mL}$.

Table S1. Speciation of Fe in Se(IV)-treated ZVI corrosion products based on LCF of Fe k^3 -weighted EXAFS spectra (Data were given as % values).

Sample ID	Material References						
	Fe ⁰	Wustite	Magnetite	Ferrihydrite	Lepidocrocite	Goethite	Maghemite
w/ SO ₄ ²⁻	19.1	20.4	43.0	9.5	8.0	--	--
w/ HSO ₃ ⁻	5.4	8.2	57.7	--	19.4	--	9.3